Eigenvalue Spectrum of MHD Modes in Cylindrical Tokamak Plasmas with Small Resistivity

Taro MATSUMOTO[1] and Shinji TOKUDA[2]

[1]*Fusion Research Development Directorate, Japan Atomic Energy Agency*

[2]*Research Organization for Information Science and Technology*

(Received: 20 November 2009 / Accepted: 5 March 2010)

For the understandings of the magnetohydrodynamic (MHD) characteristics in plasma, the spectrum of the resistive MHD modes are investigated in detail by solving the eigenvalue problem of the reduced MHD equations in cylindrical tokamak plasmas. The eigenvalues and eigenfunctions of the resistive MHD modes are clarified for small toroidal and poloidal mode numbers, and the discrete eigenvalues with imaginary part are categorized into several types by analyzing the behavior of their eigenfuctions. In particular, the dependence of the eigenvalue distribution in the real-imaginary space on the resistivity is studied for small resistivity regime by parallel computation. It is found that the characteristics of eigenvalue distribution and eigenfunction are changed even for small reduction of resistivity in small resistivity region. It is also found that the distribution structure of the eigenvalues is deformed with bifurcation of spectral curve.

Keywords: magnetohydrodynamics, stability, resistive MHD, eigenfunction, eigenvalue, tokamak, reduced MHD equations, eigenvalue problem, shear Alfven wave, parallel computation

1. Introduction

For the understandings of the tokamak plasma dynamics, it is important to investigate and clarify the characteristics of the magnetohydrodynamic (MHD) spectrum, which is also particularly important from the viewpoint of the MHD spectroscopy.

The characteristics of the MHD spectrum had been investigated by solving the eigenvalue problem based on the ideal and resistive MHD equations in cylindrical tokamak plasmas [1-2].

In the framework of the ideal MHD model, the eigenvalue problem of a MHD mode with the time dependence proportional to $e^{\lambda t}$ has one or some unstable discrete eigenvalues on the positive real axis and continuum spectrum on the imaginary axis. However, in the presence of finite plasma resistivity, it was found that the continuum spectrum is modified into purely damping spectrum on the negative real axis and discrete branches with finite imaginary and negative real components in the complex plane.

Due to the limitation of computational resources in those days, the eigenvalue distribution had been analyzed for relatively large resistivity, and the eigenfunctions of some distinguished eigenvalues was clarified.

Thus, in this paper, we have analyzed the eigenvalue distribution of cylindrical tokamak plasmas with asymptotically smaller resistivity than the previous works by using current computational resources. We have also clarified the eigenvalue distribution, its dependency on resistivity, and characteristics of eigenfunctions.

This paper is organized as follows. In Section 2, we describe our simulation method to solve the MHD problem, including the reduced MHD equations, the matrix eigenvalue problem formulation, the computational approaches and the equilibrium parameters. In Section 3, the eigenvalue distribution and the eigenfunction profile for the m/n = 1/1 and 2/1 modes are described in detail. Here m and n are the poloidal and toroidal mode number, respectively. The dependency of the eigenvalue distribution on the plasma resistivity is also shown. Finally, a brief summary is given in Sec.4.

2. Simulation Method

2.1 Basic equations

In this research, we employ a reduced MHD model where plasma can be described with the equations which do not include the fast magnetosonic wave but the shear Alfven wave. In this model, the dynamics of cylindrical plasma is described by the following reduced MHD equations for the vorticity U and the magnetic flux ψ,

$$\frac{\partial U}{\partial t} = [J,\psi]_{linear} - in\frac{B_0}{R_0}J + \nu\Delta\phi\,, \qquad (1)$$

$$\frac{\partial \psi}{\partial t} = [\psi,\phi]_{linear} - in\frac{B_0}{R_0}\phi + \eta J, \qquad (2)$$

author's e-mail: taro_matsumoto@yahoo.co.jp, matsumoto.taro@jaea.go.jp

$$U = \Delta\phi, \tag{3}$$
$$J = \Delta\psi, \tag{4}$$

which are derived from full MHD equations on the assumption of a large aspect ratio, where t is the time, ϕ is the electrostatic potential, J is the current density, η is the plasma resistivity and ν is the viscosity. Here, a cylindrical coordinates (r,θ,z) is used. The brackets in Eqs.(1) and (2) denote the linear part of the Poisson bracket,

$$[a,b] = \frac{1}{r}\left(\frac{\partial a}{\partial r}\frac{\partial b}{\partial \theta} - \frac{\partial a}{\partial \theta}\frac{\partial b}{\partial r}\right). \tag{5}$$

The delta, Δ, in Eqs.(3) and (4) denotes the Laplacian in the cylindrical coordinates, and

$$\Delta = \frac{1}{r}\frac{\partial}{\partial r}\left(r\frac{\partial}{\partial r}\right) + \frac{1}{r^2}\frac{\partial^2}{\partial \theta^2} + \frac{\partial^2}{\partial z^2}. \tag{6}$$

B_0 is the toroidal magnetic field and $2\pi R_0$ is the longitudinal length in z direction.

2.2 Formulation of matrix eigenvalue problem

The formulation of matrix eigenvalue problem is obtained from Eqs.(1) and (2) as

$$\begin{pmatrix} A_{UU} & A_{U\psi} & A_{U\phi} & A_{UJ} \\ A_{\psi U} & A_{\psi\psi} & A_{\psi\phi} & A_{\psi J} \end{pmatrix} \begin{pmatrix} U_{mn} \\ \psi_{mn} \\ \phi_{mn} \\ J_{mn} \end{pmatrix} = \lambda \begin{pmatrix} U_{mn} \\ \psi_{mn} \\ \phi_{mn} \\ J_{mn} \end{pmatrix} \tag{7}$$

where A_{XY} denotes the regular square matrix of the linear interaction, λ is a eigenvalue, and X_{mn} is a eigenfuction of physical quantity such as the vorticity U, the magnetic flux ψ, the electrostatic potential ϕ, and the current density J.

By substituting Eqs.(3) and (4) into Eq.(7), an simplified set of equations,

$$\lambda \begin{pmatrix} U_{mn} \\ \psi_{mn} \end{pmatrix} = \begin{pmatrix} A_{UU} + A_{U\phi}(\Delta^{-1}) & A_{U\psi} + A_{UJ}(\Delta) \\ A_{\psi U} + A_{\psi\phi}(\Delta^{-1}) & A_{\psi\psi} + A_{\psi J}(\Delta) \end{pmatrix} \begin{pmatrix} U_{mn} \\ \psi_{mn} \end{pmatrix} = \begin{pmatrix} A'_{UU} & A'_{U\psi} \\ A'_{\psi U} & A'_{\psi\psi} \end{pmatrix} \begin{pmatrix} U_{mn} \\ \psi_{mn} \end{pmatrix}, \tag{8}$$

is obtained, where Δ^{-1} is the inversion of the Δ of the delta. Thus, the eigenvalue problem of a restive MHD mode in a cylindrical tokamak plasma is reduced to finding the eigenvalues and eigenfunctions of Eq.(8).

2.3 Computational approach

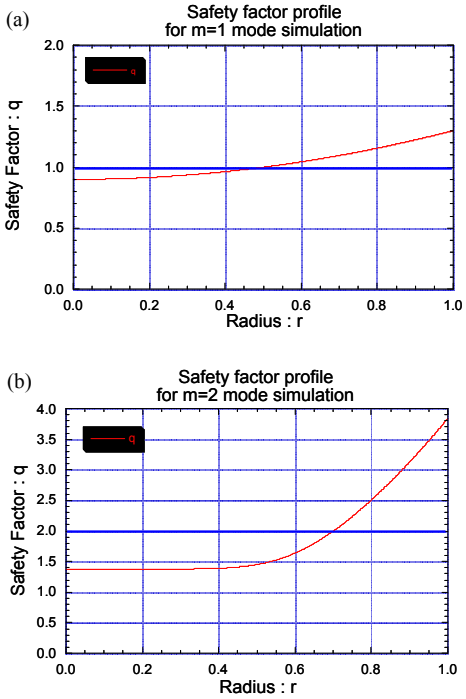

Fig.1 Safety factor profile for (a) m = 1 mode and (b) m = 2 mode.

For the numerical calculation of Eq.(8), a eigenvalue problem code has been developed. Here, at first, EISPACK is chosen as the science library for a non-parallel computation in order to solve a two-dimensional matrix. The validation of this eigenvalue problem code was confirmed by comparing with the initial value code which was independently developed, from the viewpoint of the eigenvalue (the growth rate), the eigenfunction, and grid number dependency for the m/n = 1/1 and 2/1 unstable modes.

The number of the radial grid points, i_{max}, is changed from 512 to 16385. For the large radial grid points more than 1024, the eigenvalue problem code is parallelized, and ScaLAPACK scientific library is used to solve two dimensional block cyclic distributed matrix at each processor element.

As the computational resources, we have used a workstation and SGI Altix3900 supercomputer with up to 64 processor elements. The computational time for the same eigenvalue problem is significantly reduced due to the effect of changing processor element and scientific library, and parallelization. As a result, the computational time has successfully reduced by about 4000 times.

From the viewpoint of numerical accuracy, it is found that in order to obtain precise eigenvalue distribution, good resolution should be kept over the whole radius. Thus, the uniform radial grid is used for the physical computation.

2.4 Equilibrium parameters

In this research, the safety factor profiles are assumed

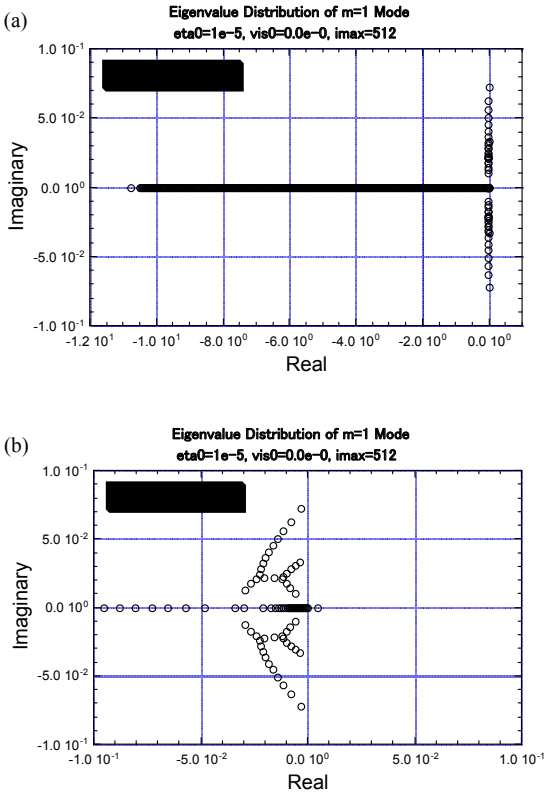

Fig.2 Eigenvalue distribution of m =1 mode in (a) macroscopic scale and (b) microscopic scale. Here, $\eta = 1.0 \times 10^{-5}$, $\nu = 0$, and $i_{max} = 512$.

as shown in Fig.1(a) and (b) for m = 1 (m/n = 1/1) mode and m=2 (m/n = 2/1) mode, respectively. The resonant magnetic surface locates at almost half plasma radius for m = 1 mode, and at approximately 0.7 of the plasma radius for m = 2 mode. For simplicity, the toroidal mode number is chosen to be 1.

The plasma resistivity η is changed from 10^{-3} to 10^{-7}. The viscosity ν is mostly assumed to be 0. However, it was confirmed that the eigenvalue distribution and the eigenfunction do not change significantly even for the viscosity equal to the plasma resistivity.

3. Characteristics of Eigenvalue Distribution and Eigenfunctions

3.1 Outline of eigenvalue distribution

At first, the macroscopic view of the eigenvalue distribution of the m = 1 mode is shown in Fig.2(a), where $\eta = 1.0 \times 10^{-5}$, $\nu = 0$, and $i_{max} = 512$. It should be noted that the scale of the real axis is 100 times larger than that of the imaginary axis to emphasize overview of the eigenvalue distribution. There are a lot of eigenvalues on the real axis in its negative region. These discrete eigenvalues indicate purely damping modes [3].

On the other hand, there are discrete eigenvalues

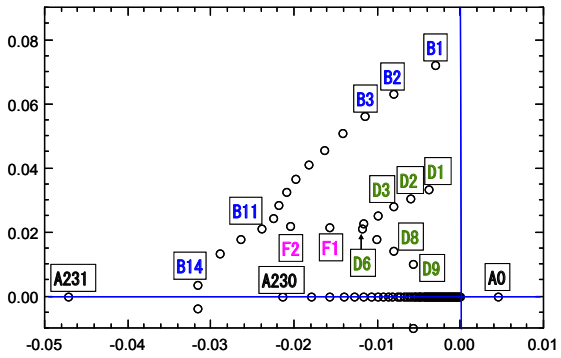

Fig.3 Detail figure of eigenvalue distribution of m = 1 mode. Here, $\eta = 1.0 \times 10^{-5}$, $\nu = 0$, and i_{max} = 512.

which situate off the real axis and have finite imaginary component and negative real component. These eigenvalues have a structure which is imaginarily symmetrical, as shown in Fig.2(b), where the scale of the real axis is almost the same to that of the imaginary axis. This structure has five branches as follows: one branch extending toward the origin, one branch extending toward the real axis, two branches towards the imaginary axis, and one branch connecting the above four branches. It is confirmed that these discrete eigenvalues do not change as the radial grid number increases while fixing physical parameters.

There is also one unstable mode on the real axis in its positive region, that is, the m = 1 kink mode, which has the eigenvalue of approximately 4×10^{-2}.

3.2 Eigenfunction of m = 1 mode

For the better understanding, the detailed figure of the eigenvalue distribution of the m=1 mode is described in Fig.3, where some characteristic eigenvalues are identified with denotations.

The eigenfunctions of D8 and D9 on the branch to the origin are shown in Fig.4(a), with A0 of the internal kink mode. The eigenfunction is normalized so that the absolute maximum value is unity. It is found that these three modes are localized in the core plasma region, namely within the resonant magnetic surface of the m = 1 mode shown in Fig.1(a). However, compared with A0, D8 and D9 have fluctuation component, in particular around the resonant surface.

The eigenfunctions of D1, D2, and D3 on the 1st branch toward the imaginary axis are shown in Fig.4(b). It is found that these modes also localize in the core plasma region, much more inward than D8, D9, and A0. It is also found that, as departing from the imaginary axis, that is, as decreasing the real component of the eigenvalue, the eigenfunction comes to have

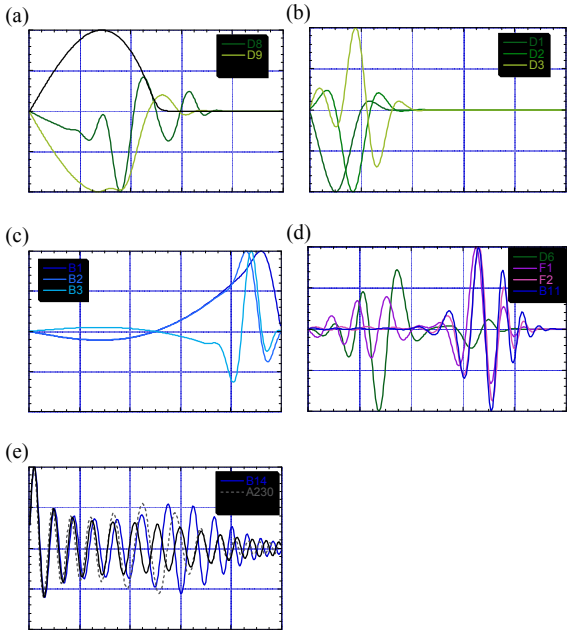

Fig.4 Eigenfunctions of m = 1 mode in (a) core-localized modes near the origin, (b) core-localized modes toward imaginary axis, (c) edge-localized modes, (d) resonant surface symmetric modes, and (e) non-localized modes. Here, η = 1.0 x 10^{-5}, ν = 0, and i_{max} = 512.

short-wavelength oscillations.

The eigenfunctions of B1, B2, and B3 on the 2nd branch toward the imaginary axis are shown in Fig.4(c). It is found that these modes localize in the edge plasma region, differently from the modes on the 1st branch toward the imaginary axis. It is also found that, as departing from the imaginary axis, the eigenfunction comes to have short-wavelength oscillations, similarly to the modes on the 1st branch toward the imaginary axis.

The eigenfunction of D6, F1, F2, and B11 on the connecting branch are shown in Fig.4(d). It is found that F1 and F2 are generally symmetrical about the resonant surface of the m = 1 mode, that is, almost zero at the resonant surface and finite fluctuation in both core and edge plasma regions. D6 has short-wavelength oscillations in the core plasma region, and on the other hand, B12 has short-wavelength oscillations in the edge plasma region.

The eigenfunction of B14 on the branch toward the real axis is shown in Fig.4(e), with A230 and A231 of the substantially damping modes. It is found that these three modes do not localize but expand uniformly in the radial direction with short-wavelength oscillations.

3.3 Eigenfunction of m = 2 mode

In order to understand the characteristics of eigenvalue and eigenfunction of a different resistive

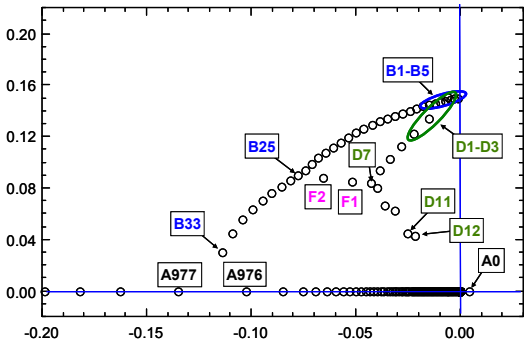

Fig.5 Detail figure of eigenvalue distribution of m = 2 mode. Here, η = 1.0 x 10^{-5}, ν = 0, and i_{max} = 2048.

MHD mode, m = 2 is chosen. The detailed figure of the eigenvalue distribution of the m = 2 mode is described in Fig.5. There are also discrete eigenvalues with imaginary component in the negative real region, which are identified with denotations, as well as Fig.3. The eigenvalue distribution has an imaginarily symmetrical structure which comprises five branches and is similar to that the m=1 mode although the 1st and 2nd branches toward the imaginary axis overlap near the imaginary axis.

There is one unstable mode, A0, on the real axis in its positive region, that is, the m = 2 tearing mode, which has the resonant magnetic surface at about r ~ 0.7 as shown in Fig.1(b) and has the eigenvalue of approximately 5 x 10^{-3}.

The eigenfunctions of D11 and D12 on the branch to the origin are shown in Fig.6(a), with the A0 of the tearing mode. It is found that these modes have fluctuation component around the resonant surface as well as Fig.4(a).

The eigenfunctions of D1, D2, and D3 on the 1st branch toward the imaginary axis are shown in Fig.6(b). It is found that these modes localize in the edge plasma region and are similar to B1 ~ B3 of the m=1 mode shown in Fig.4(c). On the other hand, the eigenfunctions of B1 ~ B5 on the 2nd branch toward the imaginary axis are shown in Fig.6(c). These modes are found to localize in the core plasma region and are similar to D1 ~D3 of the m=1 mode shown in Fig.4(b).

The eigenfunctions of D7, F1, F2, and B25 on the connecting branch, and those of B33, A976 and A977 are shown in Fig.6(d) and (e), respectively. The characteristics of D7, F1, F2, and B25, which are generally symmetrical about the resonant surface, are similar to D6, F1, F2, and B11 of the m = 1 mode as shown in Fig.4(d). The characteristics of B33, A976 and A977, which expand uniformly in the radial direction, are

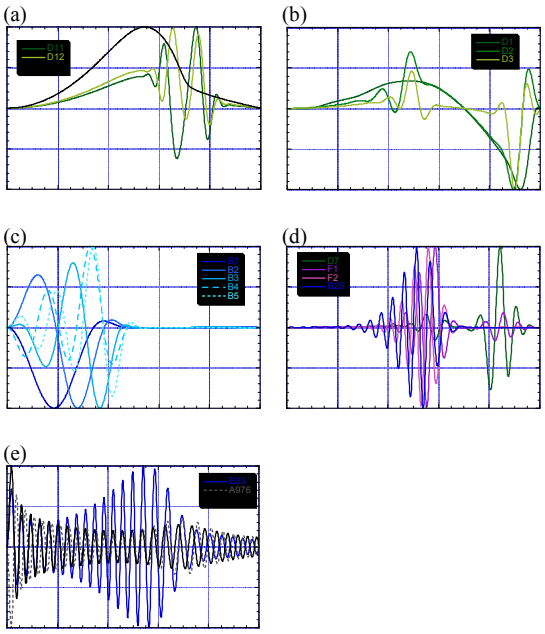

Fig.6 Eigenfunctions of m = 2 mode in (a) core-localized modes near the origin, (b) edge-localized modes toward imaginary axis, (c) core-localized modes, (d) resonant surface symmetric modes, and (e) non-localized modes. Here, $\eta = 1.0 \times 10^{-5}$, $\nu = 0$, and $i_{max} = 2048$.

similar to B33, A976 and A977 of the m = 1 mode as shown in Fig.4(e)

3.4 Dependency on plasma resistivity.

Next, in order to investigate the dependency of eigenvalue distribution on the plasma resistivity, the eigenvalue problem of the m = 1 mode is solved for different plasma resistivity. Figure 7 shows the dependency of the eigenvalues distribution of the m = 1 mode on the plasma resistivity. It is confirmed that, for a wide regime of the resistivity η from 1.0×10^{-4} to 1.5×10^{-6}, the shape and location of these curves (branches) is almost independent of the resistivity, although the density of the eigenvalues on these curves increases.

However, for further small resistivity less than 1.5×10^{-6}, it is found that the characteristics of eigenvalue distribution and eigenfunction is changed even for small reduction of resistivity, as shown in Fig.7(d) where the distribution structure is deformed with bifurcation of spectral curve.

The eigenvalue distribution of the m = 1 mode is also investigated with much larger radial grid number up to 16384, and this deformation of the eigenvalue distribution is also confirmed.

Moreover, for the much smaller resistivity, less than 1.0×10^{-6}, further deformation with bifurcation is observed. We are investigating this behavior of the

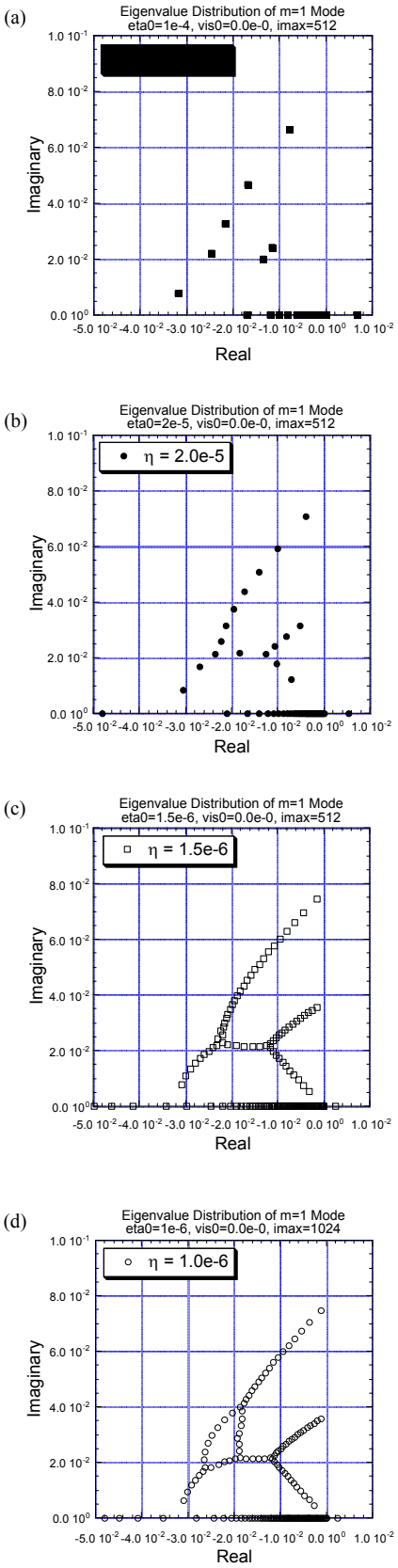

Fig.7 Eigenvalue distribution of m = 1 mode for (a) $\eta = 1.0 \times 10^{-4}$, (b) $\eta = 2.0 \times 10^{-5}$, (c) $\eta = 1.5 \times 10^{-6}$, and (d) $\eta = 1.0 \times 10^{-6}$. Here, $\nu = 0$, and i_{max} is changed from 512 to 2048.

eigenvalue distribution in detail by massively parallel computation.

4. Summary

For understandings of the MHD spectrum in a cylindrical tokamak plasma the characteristics of the $m = 1$ and $m = 2$ resistive MHD modes are investigated by solving an eigenvalue problem based on the reduced MHD model. The eigenvalue problem code was developed and was successfully parallelized for much small plasma resistivity.

The eigenvalues and eigenfunctions are clarified in detail, in particular for the structure of eigenvalue distribution which discrete eigenvalue comprise. It is confirmed that eigenvalue distribution is almost independent of the resistivity larger than 10^{-6}.

However, it is found that eigenvalue distribution is topologically deformed by reducing the resistivity to less than about 10^{-6}. It is also found that the deformation is very sensitive to small change of the resistivity in this small resistivity region.

As a future work, the WKBJ method will be applied to understand the strange phenomenon observed in Fig. 7(d). It will also be confirmed the complex spectrum is sensitive to the method used to reduce the equations [4]. The eigenvalue and eigenfunction in the inner resistive layer will be also analyzed and will be compared with those obtained by the eigenvalue problem based on the resistive MHD equations.

Acknowledgements

The authors would like to express their gratitude to Drs. M. Kikuchi, H. Ninomiya and Y. Miura (JAEA) for their useful suggestions and encouragement.

The authors would like to thank Drs. M.Yagi, N. Miyato (JAEA) and Y. Kishimoto (Kyoto Univ.) for their helpful comments.

This study was partly supported by Grant-in-Aids from the Japan Society for the Promotion of Science (No.19560832).

References

[1] W. Kerner, K. Lerbinger and K. Riedel, Phys. Fluids, **29**, 2975 (1986).

[2] B. van der Holst, A.J. Bellen, J.P. Goedbloed, et al., Phys. Plasmas, **6**, 1554 (1999).

[3] R. L. Dewar and B. Davies, J. Plasma Phys. **32**, 443 (1984)

[4] B. F. McMillan, R. L. Dewar, and R. G. Storer, Plasma Phys. Control. Fusion 46, 1027 (2004).